

FARV: LEVERAGING FACIAL AND ACOUSTIC REPRESENTATION IN VOCODER FOR VIDEO-TO-SPEECH SYNTHESIS

Anonymous authors

Paper under double-blind review

ABSTRACT

In this paper, we introduce FARV, a vocoder specifically designed for Video-to-Speech (V2S) synthesis, which integrates both facial embeddings and acoustic units to generate speech waveforms. By sharing the acoustic unit vocabulary in our two-stage V2S pipeline, FARV effectively bridges the domain gap between the visual frontend and the vocoder without requiring finetuning. Furthermore, by embedding visual speaker images into the acoustic unit representations, FARV enhances its ability to preserve speaker identity. Experimental results demonstrate that FARV achieves leading scores in intelligibility and strikes a favorable balance between speaker characteristics preservation and acoustic quality, making it well-suited for practical V2S applications¹.

1 INTRODUCTION

Video-to-Speech (V2S) synthesis (Prajwal et al., 2020a) aims to generate intelligible, natural-sounding speech directly from silent video inputs, leveraging visual cues such as lip movements and facial expressions for audio recovery. V2S is particularly useful in scenarios where only visual information is available to infer the speaker’s speech, such as in silent video meetings or for individuals who cannot produce voiced sounds.

Most V2S approaches (Mira et al., 2022; Choi et al., 2023a; Hsu et al., 2023) rely on a two-stage framework: an upstream model that extracts audio representations (Mel spectrograms or acoustic units), followed by a vocoder that converts these representations into waveforms. Since the upstream model and the vocoder are trained separately, a domain gap often arises between these two stages because the vocoder is trained on ground-truth acoustic representations from clean datasets, which may not adapt well to the outputs of the frontend encoder. Therefore, vocoders play a crucial role in V2S systems, as they are responsible for bridging the gap to upstream model outputs and recovering the audio at the same time. However, due to the drawbacks of vocoders, many existing V2S models still face significant challenges, particularly concerning the preservation of speaker identity (Hsu et al., 2023) and the generalization between synthesis stages.

Unit-based vocoders can mitigate the domain gap by sharing a common vocabulary of discrete units between the stages and can be adapted to the upstream model without concern. However, they often lose crucial speaker-specific information, resulting in synthesized audio that sounds less natural and fails to accurately reflect the original speaker’s identity. In contrast, mel-based vocoders offer better speaker preservation by utilizing Mel spectrograms, which provide richer frequency details. Yet, their sensitivity to spectral differences limits their generalization across the two stages.

To overcome these limitations, we propose an approach that combines the generalizability of unit-based vocoders with the speaker-specific preservation capabilities of mel-based vocoders. Specifically, we leverage a pre-trained facial representation extractor (Zheng et al., 2022) to capture speaker characteristics from the speaker’s image. This allows us to seamlessly integrate speaker-specific information into the vocoder. At the same time, the vocoder synthesizes audio based on acoustic units shared with the frontend encoder. This approach enables our V2S model to maintain the generaliz-

¹Code and weights will be made publicly available upon acceptance of this paper.

ability of the frontend encoder while preserving essential speaker identity features, resulting in more natural and speaker-consistent speech synthesis.

The contributions of this work can be listed as follows:

1. We introduce FARV, a unit-based vocoder that integrates facial image embeddings and acoustic units for speech synthesis, which is specifically designed for V2S.
2. FARV addresses the limitation of unit-based vocoders that struggle to retain speaker characteristics, offering a balanced approach between preserving speaker identity and ensuring high acoustic quality in V2S synthesis.
3. We demonstrate that mel-based vocoders require finetuning on frontend encoder outputs to adapt effectively to V2S. In the meantime, FARV is more resilient and can be adapted to frontend encoder even in a zero-shot manner.
4. Our V2S method achieves leading performance in acoustic intelligibility, relying solely on visual input during both training and evaluation, underscoring its practicality for real-world V2S applications.

2 RELATED WORK

2.1 VOCODERS

In speech synthesis, it is important to reconstruct speech from a compressed latent acoustic representation. To meet this need, vocoders offer a way to convert the acoustic representations to waveform. In this way, any speech-related tasks can first train a model that generates the acoustic representation, which is then fed to vocoders to synthesize speech. Vocoders are widely used in text-to-speech (TTS) (Ren et al., 2022; Shen et al., 2018; Li et al., 2019; Du et al., 2022; Jia et al., 2019; Wang et al., 2023) and have also become a favorable choice for V2S. Common choices for latent acoustic representation for vocoders are the Mel spectrogram (Kong et al., 2020; Yamamoto et al., 2020; Gil Lee et al., 2023) and the hidden unit (Polyak et al., 2021; Lee et al., 2022; Hsu et al., 2023).

While vocoders based on Mel spectrograms (mel-based vocoders) have the ability to retain speaker characteristics in speech synthesis, they are often vulnerable to domain shifts in speech conditions. For example, Chun Hsu et al. (2020) tested mel-based vocoders on unseen speakers, and have found that all tested mel-vocoders suffer from a significant domain gap. This domain gap is probably caused by the over-sensitivity of vocoders to frequency distributions of input audio, which interferes with vocoders in domain adaptations.

Later, Lee et al. (2022) found that hidden units from HuBERT (Hsu et al., 2021) can serve as an acoustic codebook to resynthesize audio waveform. Inspired by this, ReVISE (Hsu et al., 2023) proposed to use unit-HiFiGAN (unit-based vocoder) in V2S and speech enhancement. However, Hsu et al. (2023) also mentioned that HuBERT units focus on speech content and only contain knowledge capable of reconstructing utterances of spoken sentences, neglecting speaker characteristics (speaker identity like gender or age).

2.2 VIDEO TO SPEECH(V2S)

Lip2Wav (Prajwal et al., 2020a) was a pioneering work of V2S that performs speech recovery on a self-made dataset. However, Prajwal et al. (2020a) found that mel-based neural vocoders perform poorly on their generated Mel spectrograms. VAE-GAN (Hegde et al., 2022) and VCA-GAN (Kim et al., 2022) proposed adversarial learning in V2S and gained comparable performance with other supervised methods. Later, SVTS (Mira et al., 2022) tested their V2S method on LRS3 Afouras et al. (2018) and VoxCeleb2 Chung et al. (2018), which still suffers performance degradation on unseen speakers. Following SVTS, IntelligibleL2S (Choi et al., 2023b) incorporated unit and mel as vocoder input for V2S. Then, MultiTask (Kim et al., 2023) and AccurateL2S (Hegde et al., 2023) incorporated additional textual information and speaker embedding to further enhance V2S performance. However, since textual and acoustic speaker embedding is not always available, their application in practical scenarios of V2S is limited. To eliminate the need for additional inputs, DiffV2S (Choi et al., 2023a) proposed a diffusion method conditioned on visual embedding.

2.3 UNSUPERVISED FACIAL REPRESENTATION LEARNING

Unsupervised facial representation learning (Bulat et al., 2022; Zheng et al., 2022) is able to provide prior knowledge about facial identity of a person that can be transferred to downstream tasks like face attribute recognition (e.g. gender or age). Papham & Franc (2024) compared existing methods on facial gender estimation with a unified benchmark and have found that FaRL (Zheng et al., 2022) with an MLP significantly outperforms other methods thanks to the amount of data used in its pretraining. Similar to CLIP (Radford et al., 2021), FaRL is pretrained with image-text pairs on a human face subset of LAION-400M (Schuhmann et al., 2021) using contrastive loss. We therefore leverage FaRL in the training of unit-HiFiGAN to provide insights of visual speaker characteristics.

3 METHODOLOGY

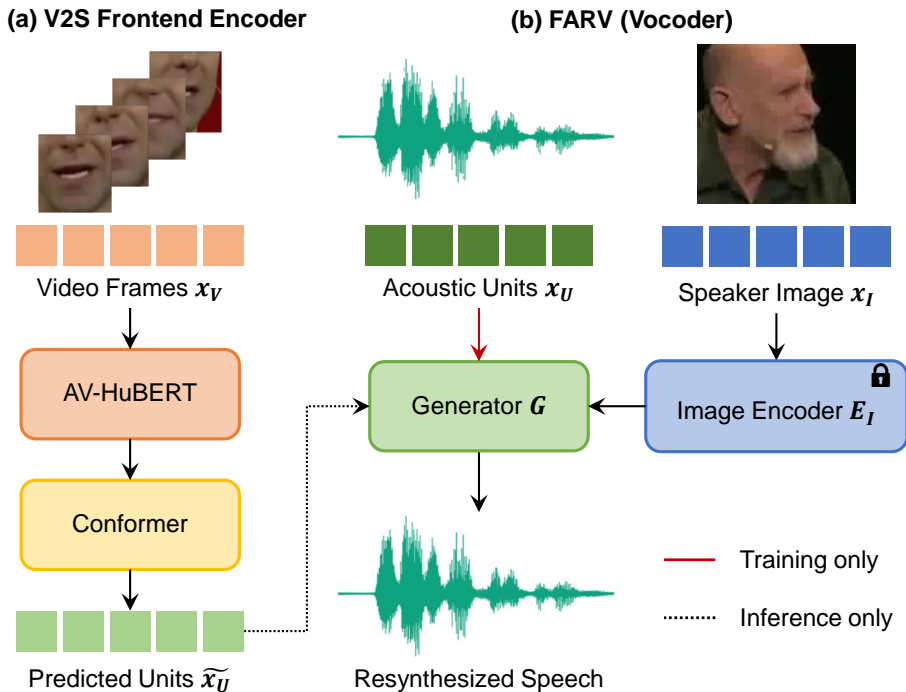


Figure 1: Overview of our V2S framework. (a) Our V2S frontend encoder is a pre-trained AV-HuBERT model followed by conformer. (b) We apply FaRL image encoder to provide visual speaker embedding for unit vocoder to preserve speaker characteristics. The proposed unit vocoder takes both acoustic units and visual embedding as input to synthesize audio.

3.1 FRAMEWORK DESIGN

Our V2S framework is a two-stage framework composing a visual frontend encoder and a vocoder. The frontend encoder utilizes a pretrained AV-HuBERT model (Shi et al., 2022a), followed by a Conformer module (Gulati et al., 2020). The AV-HuBERT model was shown to be crucial for efficient convergence in V2S tasks (Hsu et al., 2023), making it our preferred choice for the frontend backbone. To match the sampling rate of visual frames (25Hz) and that of acoustic units (50Hz), transposed convolution is applied to upsample the final output of frontend encoder. This frontend provides prior knowledge about audio-visual correlation to our V2S pipeline, offering accurate content recovery capacity.

The vocoder (FARV) is an adapted unit-HiFiGAN that combines visual embedding from the facial extractor (Zheng et al., 2022) and acoustic units. This audio-visual modality fusion will enable FARV to preserve speaker characteristics better. The acoustic units are clustered from the output of the pre-

trained HuBERT model (Hsu et al., 2021), which contains contextual information essential for the recovery of speech synthesis content. The unit vocabulary is shared for both frontend encoder and FARV.

3.2 FRONTEND ENCODER

Our frontend encoder is responsible for predicting acoustic units from silent visual inputs alone. Following ReVISE (Hsu et al., 2023), given x_V as the silent video frames and x_U as the acoustic tokens for ground-truth audio x_A , the V2S frontend is trained to produce predicted acoustic units, denoted as $f(x_V) = \tilde{x}_U$. Cross-entropy loss is adopted to optimize V2S frontend, which is formulated as

$$L_{CE} = - \sum_j^C z_j \log \text{softmax}(f(x_V))$$

, where C is the total number of classes of acoustic unit vocabulary. z_j is the one-hot indicator sequence with the ground-truth label (the j th class) of the total C acoustic classes representing x_U for each unit. During inference, we simply take the argmax of the prediction for acoustic units \tilde{x}_U as the input to the vocoder.

To create an aligned setting for testing mel-based vocoders, we also train a modified mel-based version of the frontend encoder. In this version, we adjust the training loss of the proposed method to optimize the frontend encoder using an L1 regression loss

$$L_1 = -\|M(x_A) - f(x_V)\|_1$$

, where M means Mel spectrogram conversion in logarithm. In this way, visual frontend f learns to generate Mel spectrogram. We then apply a vanilla mel-based vocoder to transfer the encoder output to audio waveform. This V2S framework is made for comparison and denoted as ReVISE (Mel).

3.3 FARV

Since unit vocoders struggle to gain speaker characteristics from acoustic units only, we apply FaRL image encoder (Zheng et al., 2022) as the visual speaker information extractor for unit-HiFiGAN to provide extra hints about speaker information. Specifically, the proposed vocoder takes both acoustic units and a visual frame cropped from the input video as input. We add the encoded image embedding from FaRL to unit embedding to provide visual guidance for speech generation. The image embedding is broadcasted to match the length of acoustic units.

For the proposed unit vocoder, given the speaker image input x_I and acoustic units x_U as input, the image encoder E_I will encode x_I to visual embedding e_I , while the lookup table for the acoustic unit vocabulary will map x_U to unit embedding e_U after convolution. During the entire training process, E_I is frozen to only produce stable facial representation embedding for unit vocoder. Then, we add these embeddings sequentially to make the fusion of audio-visual modalities p_{AV} :

$$p_{AV} = e_I \oplus e_U \quad (1)$$

p_{AV} is fed to generator G to synthesize audio. Given discriminator D (which is actually a set of discriminators (Kong et al., 2020)) and ground-truth waveform x_A , the adversarial training losses are defined as:

$$L_{adv}(D; G) = \|D(x_A) - 1\|_2 + \|D(G(p_{AV}))\|_2 \quad (2)$$

$$L_{adv}(G; D) = \|D(G(p_{AV})) - 1\|_2 \quad (3)$$

Similar to HiFiGAN, besides adversarial loss, we also Mel spectrogram loss and feature mapping loss to ensure the fidelity of synthesized audio and stabilize training:

$$L_{mel}(G) = \|M(G(p_{AV})) - M(x_A)\|_1 \quad (4)$$

$$L_{FM}(G; D) = \sum_i^T \frac{1}{N_i} \|D^i(x_A) - D^i(G(p_{AV}))\|_1 \quad (5)$$

where T denotes the number of layers in discriminator and N_i denotes the number of features on the i th layer.

The final optimization objectives for generator (L_G) and discriminator (L_D) are as follows, where λ_{mel} is a hyperparameter for loss balancing set to 45 as in Kong et al. (2020):

$$L_G = L_{adv}(G; D) + L_{FM}(G; D) + \lambda_{mel}L_{mel}(G) \quad (6)$$

$$L_D = L_{adv}(D; G) \quad (7)$$

4 EXPERIMENTS

4.1 EXPERIMENTAL SETTINGS

4.1.1 DATASETS

We applied LRS3-TED (Afouras et al., 2018) and LRS2-BBC (Afouras et al., 2022) datasets to test intelligibility of V2S systems and train the proposed vocoder. The splits of LRS3-TED are identical to that of Afouras et al. (2018). VoxCeleb2 (Chung et al., 2018) is also applied to testify equal error rate (EER) for speaker verification. All these datasets are also used to test the adaptation capability of vocoders.

We also use the audio-visual RAVDESS dataset (Livingstone & Russo, 2018) to test the capability of unit vocoders on gender and emotion classification. This is similar to the way Ji et al. (2024) tested their embedding but we only choose RAVDESS dataset of the benchmark (Livingstone & Russo, 2018) as it contains audio-visual resources. There are 8 emotions for classification² and they can be clearly reflected based on facial expression of the speaker.

4.1.2 METRICS

For low-level detail reconstruction, we utilize Extended Short-Time Objective Intelligibility (ES-TOI) and Mel Cepstral Distortion (MCD) metrics, focusing on speech intelligibility and mel-cepstral differences, respectively. To assess audio-visual synchronization, we employ LSE-C and LSE-D metrics, following the implementation from Prajwal et al. (2020b); Chung & Zisserman (2016). For content accuracy, we evaluate Word Error Rate (WER) using a pretrained ASR system (Xu et al., 2020). The wav2vec 2.0 model and weights for ASR evaluation are sourced from <https://huggingface.co/facebook/wav2vec2-large-960h-1v60-self>, identical to the setup used in ReVISE (Hsu et al., 2023). For acoustic quality, similar to how Irvin et al. (2022) evaluates vocoder, we apply NISQA-MOS (Mittag et al., 2021) to give automated non-intrusive prediction of subjective mean opinion score (MOS) scores.

For speaker characteristics preservation, we apply Speaker Encoder Cosine Similarity (SECS) and Equal Error Rate (EER) as our metrics to evaluate speaker matching performance. Following Choi et al. (2023a), we use an off-the-shelf audio speaker encoder Jia et al. (2019) for the evaluation of speaker embedding and compute SECS. EER computation is similar to Shi et al. (2022b) for speaker verification, where the matching score is the cosine similarity of speaker embedding (Jia et al., 2019) for each pair of trials. We use only one clip for each pair’s evaluation for simplicity. EER is always tested on VoxCeleb2, as speaker labels are available to construct test pairs for speaker verification.

4.1.3 TRAINING DETAILS

For all frontend encoders, we adopt the training settings from ReVISE (Hsu et al., 2023) and train the encoders on 8 GPUs for a maximum of 45,000 updates per GPU. The models are chosen based on the lowest L1 loss in the Mel spectrograms or the highest classification accuracy for the mel or unit-based frontend encoders during validation. We train ReVISE and ReVISE (Mel) frontend encoder both on our AV-HuBERT+Conformer structure for fair comparison.

For the vocoders, we follow the training setting of Hsu et al. (2023) to train HiFiGAN and unit-HiFiGAN on the single-speaker LJSpeech dataset (Ito & Johnson, 2017) resampled at 16kHz. Since visual images are required, we train FARV on the audio-visual LRS3-TED and LRS2-BBC datasets

²Emotions include neutral, calm, happy, sad, angry, fearful, disgust, surprised.

270 respectively, resuming from the checkpoint of the unit-HiFiGAN trained on LJSpeech. Vocoder
271 training is limited to a maximum of 400,000 updates across 8 GPUs, with checkpoints selected
272 based on the lowest validation loss of the Mel spectrograms.

274 4.2 V2S SYNTHESIS RESULTS

276 We compare the proposed method with existing approaches in terms of acoustic intelligibility, qual-
277 ity, and preservation of speaker characteristics in V2S synthesis. Given that finetuning on new
278 datasets can significantly compromise the acoustic quality of Unit-HiFiGAN (Section 4.3.1), we
279 utilize only the Unit-HiFiGAN model trained on LJSpeech without finetuning it on LRS2-BBC and
280 LRS3-TED for this analysis.

282 4.2.1 INTELLIGIBILITY

284 We present a comparison of baseline methods and the proposed approach for V2S in Table 1. Even
285 when only visual input is provided, the proposed method outperforms most existing approaches on
286 both the LRS3-TED and LRS2-BBC datasets, demonstrating its strong V2S synthesis capabilities.
287 Notably, while approximately half of the compared methods rely on additional acoustic speaker em-
288 beddings or textual information as supervision, which introduces out-of-domain knowledge beyond
289 visual cues in V2S training, our method consistently ranks among the top two across all evalu-
290 ated metrics. Notably, our V2S method consistently outperforms ReVISE in terms of audio-visual
291 synchronization (LSE-C and LSE-D) and low-level metrics (ESTOI and MCD), indicating superior
292 synchronization and a closer resemblance to the original audio in speech synthesis.

294 4.2.2 QUALITY AND SPEAKER CHARACTERISTICS PRESERVATION

295 We conducted a comparison between the proposed method and ReVISE on acoustic quality and
296 speaker matching in Table 2. The results demonstrate that while ReVISE achieves superior perfor-
297 mance in acoustic quality, it falls short in preserving speaker characteristics during speech synthesis.
298 In contrast, the proposed method excels in maintaining speaker characteristics. However, it is also
299 important to strike a balance between speaker characteristics preservation and acoustic quality in
300 V2S application. As discussed in Section 4.3.1, the acoustic quality of ReVISE deteriorates signif-
301 icantly while gaining improvement in speaker matching metrics after finetuning on new datasets,
302 which makes it less balanced in these two metrics.

304 4.3 VOCODER ADAPTATION CAPABILITY

306 Since the V2S frontend encoder is optimized to align with the expected inputs of the vocoder, the
307 overall synthesis performance in the V2S framework is largely constrained by the vocoder’s ca-
308 pabilities. Mel-based vocoders often face challenges in adapting to the frontend encoder’s output,
309 whereas unit-based vocoders effectively bridge this gap due to the shared acoustic unit vocabulary
310 that is consistent throughout the frontend training.

311 In the following sections, we will explore vocoder adaptation for both datasets and V2S frontend
312 applications. Dataset adaptation refers to the application of vocoders to new datasets that differ from
313 the original training data, either through fine-tuning or in a zero-shot manner. We will examine the
314 percentage drop in performance from the fine-tuned state to the zero-shot state, with smaller drops
315 indicating a vocoder’s stronger adaptability to new datasets. V2S adaptation, on the other hand,
316 focuses on evaluation of vocoders when they are applied to the output of V2S frontend encoder,
317 where domain gap may arise. We will assess the percentage drop in performance when vocoders are
318 applied in a zero-shot manner to the V2S encoder output, highlighting their practical suitability for
319 V2S applications.

320 In the following experiments, we perform finetuning for up to 400,000 updates on a single GPU,
321 selecting the model checkpoint based on the lowest validation loss of the Mel spectrogram during
322 vocoder training. FARV is further trained on the LRS3-TED dataset described in Section 4.1.3, as
323 visual images are necessary for training the proposed vocoder. In contrast, other zero-shot vocoders
are trained on the LJSpeech dataset.

LRS3-TED						
Method	Vocoder	Sync		Low-Level		Cont.
		LSE-C \uparrow	LSE-D \downarrow	ESTOI \uparrow	MCD \downarrow	WER \downarrow
<i>Methods taking visual-only input</i>						
VCA-GAN	HiFi-GAN	4.54	9.63	0.207	8.85	95.9 (Choi et al., 2023a)
DiffV2S	HiFi-GAN	<u>7.28</u>	7.27	0.284	9.35	39.2
Multi-Task	HiFi-GAN	4.85	9.15	0.240	10.16	74.8 (Choi et al., 2023a)
SVTS	HiFi-GAN	7.08	<u>7.04</u>	0.244	<u>8.60</u>	81.9 (Choi et al., 2023a)
<i>Methods requiring non-visual information</i>						
VAE-GAN \dagger	-	2.06	8.26	0.15	-	-
AccurateL2S \ddagger	BigVGAN	7.89	6.85	0.37	-	-
Multi-Task \ddagger	HiFi-GAN	5.19	8.89	0.268	9.89	65.8 (Choi et al., 2023a)
SVTS \dagger	HiFi-GAN	6.04	8.28	0.271	8.02	78.0 (Choi et al., 2023a)
<i>Our Implementation</i>						
ReVISE	Unit-HiFiGAN	7.14	7.19	<u>0.291</u>	10.68	35.67
Proposed	FARV	7.45	6.89	0.299	8.38	<u>36.81</u>
LRS2-BBC						
Method	Vocoder	Sync		Low-Level		Cont.
		LSE-C \uparrow	LSE-D \downarrow	ESTOI \uparrow	MCD \downarrow	WER \downarrow
<i>Methods taking visual-only input</i>						
VCA-GAN	HiFi-GAN	2.63	11.61	0.134	9.35	101.1 (Choi et al., 2023a)
DiffV2S	HiFi-GAN	7.51	9.81	0.283	9.85	52.7
Multi-Task	HiFi-GAN	7.19	7.01	<u>0.322</u>	10.22	61.0 (Choi et al., 2023a)
SVTS	HiFi-GAN	<u>7.87</u>	6.30	0.301	<u>7.97</u>	76.6 (Choi et al., 2023a)
<i>Methods requiring non-visual information</i>						
VAE-GAN \dagger	-	2.51	8.16	0.17	-	-
AccurateL2S \ddagger	BigVGAN	8.08	6.59	0.47	-	-
Multi-Task \ddagger	HiFi-GAN	6.88	7.32	0.341	9.37	57.8 (Choi et al., 2023a)
SVTS \dagger	HiFi-GAN	7.80	6.47	0.331	6.86	71.4 (Choi et al., 2023a)
<i>Our Implementation</i>						
ReVISE	Unit-HiFiGAN	7.48	6.79	0.300	11.05	<u>37.65</u>
Proposed	FARV	7.92	<u>6.34</u>	0.331	7.91	34.75

Table 1: Intelligibility evaluation on the LRS3-TED and LRS2-BBC datasets. Top-1 and top-2 performances for methods using visual-only input are highlighted in bold and underlined, respectively. Methods marked with \dagger require additional speaker embeddings during training, while those marked with \ddagger utilize both audio embeddings and supplementary textual information.

Method	LRS3-TED		LRS2-BBC	
	Match	Qual.	Match	Qual.
	SECS \uparrow	NISQA-MOS \uparrow	SECS \uparrow	NISQA-MOS \uparrow
ReVISE	53.93	4.10	52.31	3.98
Proposed	61.23	2.76	62.34	2.31

Table 2: Speaker matching scores for evaluating speaker characteristics preservation on the LRS2-BBC and LRS3-TED datasets.

4.3.1 DATASET ADAPTATION AND FINETUNING OF VOCODERS

In this section, we present the percentage of performance degradation observed in unit-based and mel-based vocoders when adapting to different datasets. The evaluation is conducted under both zero-shot and finetuned conditions to assess the generalization capabilities of these vocoders across various datasets.

We can observe from Table 3 that unit-based vocoders exhibit generally more stable performance on low-level metrics compared to mel-based vocoders in a zero-shot scenario, highlighting the inherent consistency of acoustic intelligibility in unit-based vocoders across different datasets. However, because unit-HiFiGAN is trained on a single-speaker LJSpeech dataset and encodes only the acoustic information relevant to speech content, it demonstrates the worst speaker matching performance in the zero-shot scenario. Additionally, as illustrated in Figure 2, unit-HiFiGAN experiences a signif-

378 icant decline in acoustic quality when finetuned on new datasets. This degradation may be due to
 379 its unit vocabulary, which is effective for preserving acoustic content but insufficient for encoding
 380 diverse speaker information.

381 FARV outperforms vanilla unit-HiFiGAN across all metrics, particularly in preserving speaker char-
 382 acteristics, with the only exception being acoustic quality in zero-shot settings. However, when both
 383 FARV and unit-HiFiGAN are finetuned on a new dataset, FARV consistently achieves better per-
 384 formance. As shown in Figure 2, the low drop rates in performance further demonstrate FARV’s
 385 superior generalizability.

Vocoder Input: GT Acoustic Representation

Finetuned	Vocoder	Match		Qual.	Low-Level	
		SECS↑	EER↓	NISQA-MOS↑	ESTOI↑	MCD↓
LRS2-BBC						
✓	HiFiGAN	94.71	20.62	2.81	0.863	1.57
	Unit-HiFiGAN	61.96	37.26	2.21	0.412	7.66
	FARV	<u>65.16</u>	<u>30.52</u>	<u>2.35</u>	<u>0.464</u>	<u>7.25</u>
×	HiFiGAN	87.84	24.02	2.47	0.805	2.29
	Unit-HiFiGAN	52.69	41.08	4.07	0.417	10.24
	FARV	<u>60.23</u>	<u>28.36</u>	<u>2.64</u>	<u>0.440</u>	<u>7.94</u>
VoxCeleb2						
✓	HiFiGAN	95.67	19.76	2.94	0.821	1.62
	Unit-HiFiGAN	61.98	37.29	2.29	0.374	7.93
	FARV	<u>63.94</u>	<u>29.28</u>	<u>2.48</u>	<u>0.393</u>	<u>7.57</u>
×	HiFiGAN	84.26	24.02	2.34	0.740	2.53
	Unit-HiFiGAN	48.18	41.08	4.16	0.372	10.75
	FARV	<u>60.95</u>	<u>28.36</u>	<u>2.87</u>	<u>0.400</u>	<u>7.92</u>

Table 3: Dataset finetuning results where zero-shot vocoder adaptation is compared with its fine-tuned counterpart on the LRS2 and VoxCeleb2 test sets.

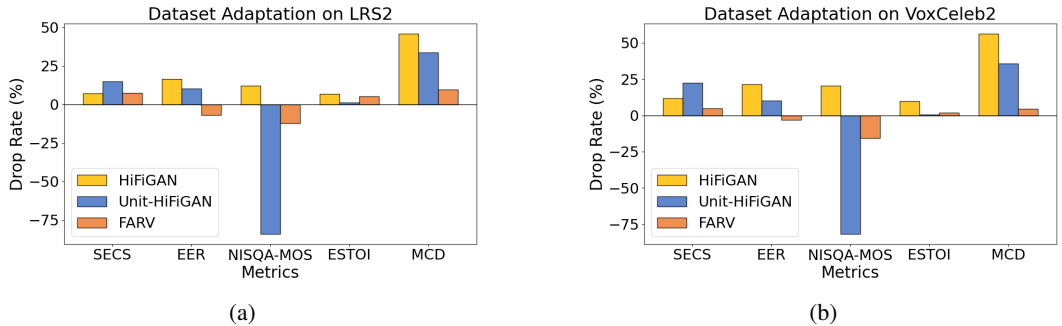


Figure 2: Performance drop rates of dataset adaptation on (a) LRS2-BBC dataset; (b) VoxCeleb2 dataset. The drop rates are presented as relative percentages, highlighting the domain gap between finetuned and zero-shot vocoders. Positive values indicate a performance drop, while negative values demonstrate that zero-shot performance is superior to that of the finetuned model.

4.3.2 FRONTEND ADAPTATION OF VOCODERS IN V2S

385 Since vocoders are ultimately used with frontend encoders for V2S applications, we explore the
 386 adaptability of different vocoders when used in conjunction with the frontend encoder. We present
 387 the evaluation of audio quality generated by vocoders that have not been finetuned on the frontend
 388 encoder output, using this as a baseline to assess their ability to recover audio from the frontend
 389 encoder within the V2S framework.

390 Table 4 and Figure 3 show that mel-based vocoders experience a much more significant drop in per-
 391 formance compared to unit-based vocoders when adapting to V2S frontend encoders. Specifically,
 metrics related to speaker matching, quality, and low-level features degrade significantly regardless

of whether the vocoders are finetuned on the LRS2-BBC dataset. This is likely due to frequency domain differences. As a result, the advantages mel-based vocoders demonstrate during training with ground-truth inputs are diminished in this scenario, highlighting the necessity of unit-based vocoders in V2S applications, especially when finetuning vocoders is not feasible.

Vocoder Input: V2S frontend prediction

Finetuned	Vocoder	Match		Qual.	Low-Level	
		SECS \uparrow	EER \downarrow	NISQA-MOS \uparrow	ESTOI \uparrow	MCD \downarrow
×	HiFiGAN	<u>57.52</u>	<u>33.67</u>	1.00	0.376	7.53
	Unit-HiFiGAN	52.31	42.53	3.98	0.300	10.88
	FARV	58.57	30.01	<u>2.64</u>	<u>0.311</u>	<u>8.75</u>
✓	HiFiGAN	58.83	<u>34.47</u>	1.06	0.375	7.59
	Unit-HiFiGAN	<u>59.88</u>	37.59	<u>2.28</u>	0.312	8.68
	FARV	63.08	31.30	2.30	<u>0.330</u>	<u>8.15</u>

Table 4: Frontend adaptation results when paired with the frontend encoder for V2S synthesis on the LRS2-BBC dataset. Vocoders labeled as "Finetuned" are trained on ground-truth audio from the LRS2-BBC dataset rather than the predicted outputs from the frontend encoder.

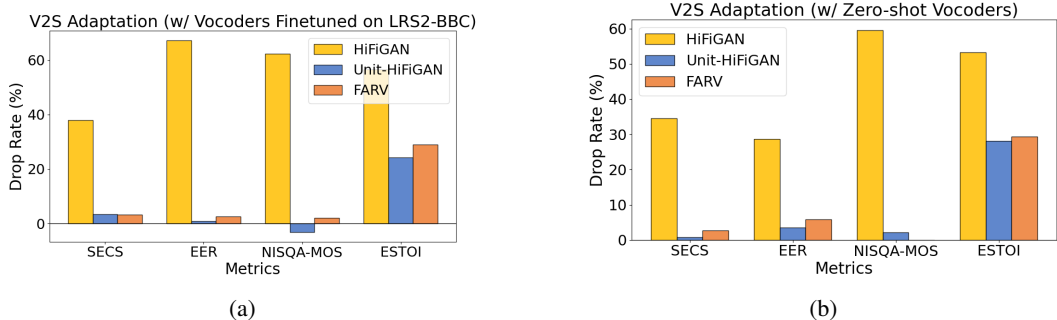


Figure 3: Performance drop rates of V2S adaptation evaluated on the LRS2-BBC dataset. The vocoders used are (a) finetuned on the LRS2-BBC dataset and (b) applied in a zero-shot manner. The drop rates are presented as relative percentages, comparing the ground-truth acoustic representation to the predictions from the V2S frontend encoder, which serve as input for the vocoders.

4.3.3 FINETUNING ON FRONTEND OUTPUT FOR MEL-BASED VOCODERS

Updates	Sync		Match		Low-Level		Qual.	Cont.
	LSE-C \uparrow	LSE-D \downarrow	SECS \uparrow	EER \downarrow	ESTOI \uparrow	MCD \downarrow	NISQA-MOS \uparrow	WER \downarrow
0k	7.14	7.13	53.91	32.31	0.333	7.73	1.07	<u>35.45</u>
200k	7.86	<u>6.56</u>	<u>60.76</u>	<u>30.01</u>	0.333	7.94	<u>2.62</u>	34.61
500k	<u>7.83</u>	6.54	60.99	29.14	<u>0.326</u>	<u>7.77</u>	2.73	35.68

Table 5: Effect of the mel vocoder (HiFiGAN) finetuned on Mel spectrograms generated by the trained ReVISE (mel) model in the LRS3-TED dataset. The differences indicate the number of finetuning updates applied to the vocoder, where "0k" signifies that HiFiGAN is trained on LJSpeech without any finetuning (zero-shot)

In Section 4.3.2, we can observe that HiFiGAN incurs a significant drop in performance when adapted to the V2S frontend encoder in a zero-shot manner. Therefore, it is necessary to finetune HiFiGAN on Mel spectrograms generated by a fully trained frontend encoder to help it adapt to the domain gap. The results in Table 5 reveal a substantial improvement in acoustic quality after finetuning the vocoder on Mel spectrograms generated from the encoder output. Metrics for speaker matching and audio-visual synchronization also improve after finetuning, indicating a considerable performance gap induced by the domain gap for HiFiGAN when adapting to the V2S frontend encoder. Since practical V2S applications require converting visual inputs into speech, where audio is

often unavailable after deployment, this poses a significant limitation for using mel-based vocoders in V2S.

Therefore, while the mel-based vocoder maintains favorable performance across many metrics on different datasets (as shown in Table 3), it is still affected by the domain gap in V2S, making fine-tuning on frontend encoder outputs necessary for practical use. In contrast, unit-based vocoders can be applied to V2S in a zero-shot manner without requiring finetuning on model outputs, as they only predict acoustic units from a shared vocabulary used during the training of both the vocoder and the V2S frontend encoder.

4.4 EMBEDDING CAPABILITY

To testify the capability of the proposed method against traditional unit-HiFiGAN, we conducted experiments on unit embedding of these two vocoders. We train a simple baseline where a linear classifier is required to perform classification on gender and emotion. The linear model takes the output of unit embedding as input. During the entire training process of the classification baseline, the vocoder remains frozen and only provides embedding outputs to feed the linear classifier.

Task	Model	Micro Acc (%)
Emotion	FARV	69.44
	Unit-HiFiGAN	45.14
Gender	FARV	100.00
	Unit-HiFiGAN	81.94

Table 6: Micro accuracy for emotion and gender tasks.

Table 6 shows the results of the linear classification given different embeddings of the vocoder as input. When unit embedding of the proposed method are given, the accuracy of gender or emotion classification improves significantly compared to its unit-only counterpart. Notably, gender classification archives 100% accuracy for the proposed method, while unit-HiFiGAN fails to eliminate the ambiguity of speaker gender identity.

5 CONCLUSION

In this paper, we introduced FARV, a vocoder specifically designed for Video-to-Speech (V2S) synthesis that effectively integrates audio-visual modalities. Through a comparative analysis with existing vocoders, we identified their key limitations: mel-based vocoders struggle to adapt to the outputs of V2S frontend encoders, which limits their practical applicability, while unit-based vocoders face challenges in balancing speaker identity preservation with acoustic quality. FARV addresses these issues by incorporating facial image embeddings, which enhance the preservation of speaker characteristics, and by utilizing a shared unit vocabulary that seamlessly integrates with the V2S pipeline. Experimental results demonstrate that FARV achieves superior intelligibility and strikes an advantageous balance between preserving speaker characteristics and maintaining sound quality, even when adapted to new datasets. Overall, FARV shows significant potential for practical V2S applications, effectively minimizing the performance drops typically observed in mel-based approaches.

REFERENCES

- Triantafyllos Afouras, Joon Son Chung, and Andrew Zisserman. Lrs3-ted: a large-scale dataset for visual speech recognition. *ArXiv*, abs/1809.00496, 2018. URL <https://api.semanticscholar.org/CorpusID:52155419>.
- Triantafyllos Afouras, Joon Son Chung, Andrew Senior, Oriol Vinyals, and Andrew Zisserman. Deep audio-visual speech recognition. *IEEE Transactions on Pattern Analysis and Machine Intelligence*, 44(12):8717–8727, December 2022. ISSN 1939-3539. doi: 10.1109/tpami.2018.2889052. URL <http://dx.doi.org/10.1109/TPAMI.2018.2889052>.

- 540 Adrian Bulat, Shiyang Cheng, Jing Yang, Andrew Garbett, Enrique Sanchez, and Georgios Tz-
541 imiropoulos. Pre-training strategies and datasets for facial representation learning, 2022. URL
542 <https://arxiv.org/abs/2103.16554>.
- 543
- 544 Jeongsoo Choi, Joanna Hong, and Yong Man Ro. Diffv2s: Diffusion-based video-to-speech synthe-
545 sis with vision-guided speaker embedding, 2023a.
- 546 Jeongsoo Choi, Minsu Kim, and Yong Man Ro. Intelligible lip-to-speech synthesis with speech
547 units, 2023b.
- 548
- 549 Po chun Hsu, Chun hsuan Wang, Andy T. Liu, and Hung yi Lee. Towards robust neural vocoding
550 for speech generation: A survey, 2020. URL <https://arxiv.org/abs/1912.02461>.
- 551
- 552 J. S. Chung and A. Zisserman. Out of time: automated lip sync in the wild. In *Workshop on*
553 *Multi-view Lip-reading, ACCV*, 2016.
- 554 Joon Son Chung, Arsha Nagrani, and Andrew Zisserman. Voxceleb2: Deep speaker recogni-
555 tion. In *Interspeech*, 2018. URL [https://api.semanticscholar.org/CorpusID:](https://api.semanticscholar.org/CorpusID:49211906)
556 [49211906](https://api.semanticscholar.org/CorpusID:49211906).
- 557
- 558 Chenpeng Du, Yiwei Guo, Xie Chen, and K. Yu. Vqts: High-fidelity text-to-speech synthesis
559 with self-supervised vq acoustic feature. *ArXiv*, abs/2204.00768, 2022. URL [https://api.](https://api.semanticscholar.org/CorpusID:247939783)
560 [semanticscholar.org/CorpusID:247939783](https://api.semanticscholar.org/CorpusID:247939783).
- 561 Sang gil Lee, Wei Ping, Boris Ginsburg, Bryan Catanzaro, and Sungroh Yoon. Bigvgan: A universal
562 neural vocoder with large-scale training, 2023.
- 563
- 564 Anmol Gulati, James Qin, Chung-Cheng Chiu, Niki Parmar, Yu Zhang, Jiahui Yu, Wei Han,
565 Shibo Wang, Zhengdong Zhang, Yonghui Wu, and Ruoming Pang. Conformer: Convolution-
566 augmented transformer for speech recognition. *ArXiv*, abs/2005.08100, 2020. URL [https:](https://api.semanticscholar.org/CorpusID:218674528)
567 [//api.semanticscholar.org/CorpusID:218674528](https://api.semanticscholar.org/CorpusID:218674528).
- 568 Sindhu B. Hegde, K R Prajwal, Rudrabha Mukhopadhyay, Vinay P. Namboodiri, and C.V. Jawahar.
569 Lip-to-speech synthesis for arbitrary speakers in the wild. In *Proceedings of the 30th ACM In-*
570 *ternational Conference on Multimedia*, MM '22. ACM, October 2022. doi: 10.1145/3503161.
571 3548081. URL <http://dx.doi.org/10.1145/3503161.3548081>.
- 572
- 573 Sindhu B. Hegde, Rudrabha Mukhopadhyay, C. V. Jawahar, and Vinay Namboodiri. Towards ac-
574 curate lip-to-speech synthesis in-the-wild. *Proceedings of the 31st ACM International Confer-*
575 *ence on Multimedia*, 2023. URL [https://api.semanticscholar.org/CorpusID:](https://api.semanticscholar.org/CorpusID:264492689)
576 [264492689](https://api.semanticscholar.org/CorpusID:264492689).
- 577 Wei-Ning Hsu, Benjamin Bolte, Yao-Hung Hubert Tsai, Kushal Lakhotia, Ruslan Salakhutdinov,
578 and Abdelrahman Mohamed. Hubert: Self-supervised speech representation learning by masked
579 prediction of hidden units. *IEEE/ACM Transactions on Audio, Speech, and Language Processing*,
580 29:3451–3460, 2021. doi: 10.1109/TASLP.2021.3122291.
- 581
- 582 Wei-Ning Hsu, Tal Remez, Bowen Shi, Jacob Donley, and Yossi Adi. Revise: Self-supervised
583 speech resynthesis with visual input for universal and generalized speech regeneration. In *2023*
584 *IEEE/CVF Conference on Computer Vision and Pattern Recognition (CVPR)*, pp. 18796–18806,
585 2023. doi: 10.1109/CVPR52729.2023.01802.
- 586 Bryce Irvin, Marko Stamenovic, Mikolaj Kegler, and Li-Chia Yang. Self-supervised learning for
587 speech enhancement through synthesis, 2022. URL [https://arxiv.org/abs/2211.](https://arxiv.org/abs/2211.02542)
588 [02542](https://arxiv.org/abs/2211.02542).
- 589 Keith Ito and Linda Johnson. The lj speech dataset. [https://keithito.com/](https://keithito.com/LJ-Speech-Dataset/)
590 [LJ-Speech-Dataset/](https://keithito.com/LJ-Speech-Dataset/), 2017.
- 591
- 592 Shengpeng Ji, Ziyue Jiang, Xize Cheng, Yifu Chen, Minghui Fang, Jialong Zuo, Qian Yang, Ruiqi
593 Li, Ziang Zhang, Xiaoda Yang, et al. Wavtokenizer: an efficient acoustic discrete codec tokenizer
for audio language modeling. *arXiv preprint arXiv:2408.16532*, 2024.

- 594 Ye Jia, Yu Zhang, Ron J. Weiss, Quan Wang, Jonathan Shen, Fei Ren, Zhifeng Chen, Patrick
595 Nguyen, Ruoming Pang, Ignacio Lopez Moreno, and Yonghui Wu. Transfer learning from speaker
596 verification to multispeaker text-to-speech synthesis, 2019.
- 597 Minsu Kim, Joanna Hong, and Yong Man Ro. Lip to speech synthesis with visual context
598 attentional gan. In *Neural Information Processing Systems*, 2022. URL [https://api.
599 semanticscholar.org/CorpusID:247957894](https://api.semanticscholar.org/CorpusID:247957894).
- 600 Minsu Kim, Joanna Hong, and Yong Man Ro. Lip-to-speech synthesis in the wild with multi-task
601 learning. *ICASSP 2023 - 2023 IEEE International Conference on Acoustics, Speech and Sig-
602 nal Processing (ICASSP)*, pp. 1–5, 2023. URL [https://api.semanticscholar.org/
603 CorpusID:257019598](https://api.semanticscholar.org/CorpusID:257019598).
- 604 Davis E. King. Dlib-ml: A machine learning toolkit. *J. Mach. Learn. Res.*, 10:1755–1758, dec 2009.
605 ISSN 1532-4435.
- 606 Jungil Kong, Jaehyeon Kim, and Jaekyoung Bae. Hifi-gan: Generative adversarial networks for
607 efficient and high fidelity speech synthesis, 2020.
- 608 Ann Lee, Peng-Jen Chen, Changhan Wang, Jiatao Gu, Sravya Popuri, Xutai Ma, Adam Polyak,
609 Yossi Adi, Qing He, Yun Tang, Juan Pino, and Wei-Ning Hsu. Direct speech-to-speech transla-
610 tion with discrete units. In Smaranda Muresan, Preslav Nakov, and Aline Villavicencio (eds.),
611 *Proceedings of the 60th Annual Meeting of the Association for Computational Linguistics (Vol-
612 ume 1: Long Papers)*, pp. 3327–3339, Dublin, Ireland, May 2022. Association for Computational
613 Linguistics. doi: 10.18653/v1/2022.acl-long.235. URL [https://aclanthology.org/
614 2022.acl-long.235](https://aclanthology.org/2022.acl-long.235).
- 615 Naihuan Li, Shujie Liu, Yanqing Liu, Sheng Zhao, Ming Liu, and Ming Zhou. Neural speech synthe-
616 sis with transformer network, 2019. URL <https://arxiv.org/abs/1809.08895>.
- 617 Steven R. Livingstone and Frank A. Russo. The ryerson audio-visual database of emotional speech
618 and song (ravdess): A dynamic, multimodal set of facial and vocal expressions in north american
619 english. *PLOS ONE*, 13(5):1–35, 05 2018. doi: 10.1371/journal.pone.0196391. URL [https:
620 //doi.org/10.1371/journal.pone.0196391](https://doi.org/10.1371/journal.pone.0196391).
- 621 Rodrigo Mira, Alexandros Haliassos, Stavros Petridis, Björn W. Schuller, and Maja Pantic. Svts:
622 Scalable video-to-speech synthesis, 2022.
- 623 Gabriel Mittag, Babak Naderi, Assmaa Chehadi, and Sebastian Möller. Nisqa: A deep cnn-self-
624 attention model for multidimensional speech quality prediction with crowdsourced datasets. In
625 *Interspeech 2021*, interspeech2021.ISCA, August 2021. doi : . URL [http://dx.doi.org/
626 10.21437/Interspeech.2021-299](http://dx.doi.org/10.21437/Interspeech.2021-299).
- 627 Vassil Panayotov, Guoguo Chen, Daniel Povey, and Sanjeev Khudanpur. Librispeech: An asr corpus
628 based on public domain audio books. In *2015 IEEE International Conference on Acoustics, Speech
629 and Signal Processing (ICASSP)*, pp. 5206–5210, 2015. 10.1109/ICASSP.2015.7178964.
- 630 Jakub Paplham and Vojtech Franc. A call to reflect on evaluation practices for age estimation:
631 Comparative analysis of the state-of-the-art and a unified benchmark, 2024. URL [https://
632 arxiv.org/abs/2307.04570](https://arxiv.org/abs/2307.04570).
- 633 Adam Polyak, Yossi Adi, Jade Copet, Eugene Kharitonov, Kushal Lakhota, Wei-Ning Hsu, Abdel
634 rahman Mohamed, and Emmanuel Dupoux. Speech resynthesis from discrete disentangled self-
635 supervised representations. In *Interspeech*, 2021. URL [https://api.semanticscholar.
636 org/CorpusID:262491522](https://api.semanticscholar.org/CorpusID:262491522).
- 637 K R Prajwal, Rudrabha Mukhopadhyay, Vinay Namboodiri, and C V Jawahar. Learning individual
638 speaking styles for accurate lip to speech synthesis, 2020a.
- 639 K R Prajwal, Rudrabha Mukhopadhyay, Vinay P. Namboodiri, and C.V. Jawahar. A lip sync expert
640 is all you need for speech to lip generation in the wild. In *Proceedings of the 28th ACM International
641 Conference on Multimedia, MM '20*, pp. 484–492, New York, NY, USA, 2020b. Association for
642 Computing Machinery. ISBN 9781450379885. 10.1145/3394171.3413532. URL [https://
643 doi.org/10.1145/3394171.3413532](https://doi.org/10.1145/3394171.3413532).

- 648 Alec Radford, Jong Wook Kim, Chris Hallacy, Aditya Ramesh, Gabriel Goh, Sandhini Agarwal,
649 Girish Sastry, Amanda Askell, Pamela Mishkin, Jack Clark, Gretchen Krueger, and Ilya Sutskever.
650 Learning transferable visual models from natural language supervision, 2021. URL [https://](https://arxiv.org/abs/2103.00020)
651 arxiv.org/abs/2103.00020.
- 652 Yi Ren, Chenxu Hu, Xu Tan, Tao Qin, Sheng Zhao, Zhou Zhao, and Tie-Yan Liu. FastSpeech 2:
653 Fast and high-quality end-to-end text to speech, 2022.
- 654 Christoph Schuhmann, Richard Vencu, Romain Beaumont, Robert Kaczmarczyk, Clayton Mullis,
655 Aarush Katta, Theo Coombes, Jenia Jitsev, and Aran Komatsuzaki. Laion-400m: Open dataset
656 of clip-filtered 400 million image-text pairs, 2021. URL [https://arxiv.org/abs/2111.](https://arxiv.org/abs/2111.02114)
657 [02114](https://arxiv.org/abs/2111.02114).
- 658 Jonathan Shen, Ruoming Pang, Ron J. Weiss, Mike Schuster, Navdeep Jaitly, Zongheng Yang,
659 Zhifeng Chen, Yu Zhang, Yuxuan Wang, RJ Skerry-Ryan, Rif A. Saurous, Yannis Agiomyrgian-
660 nakis, and Yonghui Wu. Natural tts synthesis by conditioning wavenet on mel spectrogram predic-
661 tions, 2018. URL <https://arxiv.org/abs/1712.05884>.
- 662 Bowen Shi, Wei-Ning Hsu, Kushal Lakhota, and Abdel rahman Mohamed. Learning audio-visual
663 speech representation by masked multimodal cluster prediction. *ArXiv*, abs/2201.02184, 2022a.
664 URL <https://api.semanticscholar.org/CorpusID:245769552>.
- 665 Bowen Shi, Abdel rahman Mohamed, and Wei-Ning Hsu. Learning lip-based audio-visual
666 speaker embeddings with av-hubert. *ArXiv*, abs/2205.07180, 2022b. URL [https://api.](https://api.semanticscholar.org/CorpusID:248810864)
667 [semanticscholar.org/CorpusID:248810864](https://api.semanticscholar.org/CorpusID:248810864).
- 668 Benjamin van Niekerk, Marc-André Carbonneau, Julian Zaïdi, Matthew Baas, Hugo Seuté, and
669 Herman Kamper. A comparison of discrete and soft speech units for improved voice conver-
670 sion. *ICASSP 2022 - 2022 IEEE International Conference on Acoustics, Speech and Signal Pro-*
671 *cessing (ICASSP)*, pp. 6562–6566, 2021. URL [https://api.semanticscholar.org/](https://api.semanticscholar.org/CorpusID:241033084)
672 [CorpusID:241033084](https://api.semanticscholar.org/CorpusID:241033084).
- 673 Chengyi Wang, Sanyuan Chen, Yu Wu, Ziqiang Zhang, Long Zhou, Shujie Liu, Zhuo Chen, Yanqing
674 Liu, Huaming Wang, Jinyu Li, Lei He, Sheng Zhao, and Furu Wei. Neural codec language mod-
675 els are zero-shot text to speech synthesizers, 2023. URL [https://arxiv.org/abs/2301.](https://arxiv.org/abs/2301.02111)
676 [02111](https://arxiv.org/abs/2301.02111).
- 677 Qiantong Xu, Alexei Baevski, Tatiana Likhomanenko, Paden Tomaso, Alexis Conneau, Ronan
678 Collobert, Gabriel Synnaeve, and Michael Auli. Self-training and pre-training are complemen-
679 tary for speech recognition. *ICASSP 2021 - 2021 IEEE International Conference on Acous-*
680 *tics, Speech and Signal Processing (ICASSP)*, pp. 3030–3034, 2020. URL [https://api.](https://api.semanticscholar.org/CorpusID:225039936)
681 [semanticscholar.org/CorpusID:225039936](https://api.semanticscholar.org/CorpusID:225039936).
- 682 Ryuichi Yamamoto, Eunwoo Song, and Jae-Min Kim. Parallel wavegan: A fast waveform genera-
683 tion model based on generative adversarial networks with multi-resolution spectrogram. In *ICASSP*
684 *2020 - 2020 IEEE International Conference on Acoustics, Speech and Signal Processing (ICASSP)*,
685 pp. 6199–6203, 2020. 10.1109/ICASSP40776.2020.9053795.
- 686 Yinglin Zheng, Hao Yang, Ting Zhang, Jianmin Bao, Dongdong Chen, Yangyu Huang, Lu Yuan,
687 Dong Chen, Ming Zeng, and Fang Wen. General facial representation learning in a visual-linguistic
688 manner, 2022. URL <https://arxiv.org/abs/2112.03109>.

694 A DETAILED EXPERIMENTAL SETUP

697 A.1 AUDIO-VISUAL DATASET SETUP

698 For audio-visual datasets, we use the official splits of LRS2-BBC. As LRS3-TED does not have
699 official validation set, we apply the validation split provided by AV-HuBERT (Shi et al., 2022a). All
700 resource in audio-visual datasets is used (224 hours for LRS2-BBC and 433 hours for LRS3-TED)
701 to train V2S framework.

A.2 CONFIGURATION

K-Means clustering with 2000 categories on the third iteration feature from the last layer of the HuBERT model Hsu et al. (2021) is applied to all our training dataset to build the acoustic unit vocabulary shared by both the frontend encoder and the vocoder. The HuBERT model for clustering is the BASE version pretrained on 960 hours of the LibriSpeech dataset Panayotov et al. (2015). The frontend encoder comprises AV-HuBERT LARGE of 325M parameters along with a 4-block conformer module. The conformer has 4 attention heads with attention dimension of 256 and has 11M parameters for adapting visual input to acoustic representation prediction.

For the frontend encoder, we follow Shi et al. (2022a) to preprocess the visual input, as the upstream visual frontend uses an AV-HuBERT model. Preprocessing ensure that video frames are cropped to 96x96 based on facial keypoints detected by the dlib tool King (2009) and transformed into grayscale frames after an affine transformation. In acutal use of model, we further crop it to an area of 88x88 pixel region. During training, visual frames have a 50% chance of being horizontally flipped and are limited to 4.0 seconds from the start of each video. For evaluation, we consistently apply a center crop without flipping, and load the entire video into the model.

For FARV, we crop the speaker image at the middle frame of raw input video (unpreprocessed) in RGB and apply transformation identical to FaRL (Zheng et al., 2022) which applies center-crop to 224x224 to input RGB image after bicubic interpolation. We then normalize the image in RGB which is ready as the input to FaRL image encoder. No facial crop is performed as FaRL is trained on LAION-Face (Zheng et al., 2022), a dataset that contains human facial image-text pairs with the human face showing up at varied positions of different angles in image, which brings it the capability of zero-shot adaptation.

For Mel spectrogram generation during vocoder training and the ReVISE (Mel) frontend encoder, we follow van Niekerk et al. (2021), extracting 128-dimensional Mel spectrograms from raw audio at 10-ms intervals across all datasets. Since all our dataset has acoustic sampling rate of 16kHz, the hop size is set to 160, aligning with the upsampled visual features (100FPS after upsampling 4 times from 25Hz of original video clips). Size of fft is set to be 512.

A.3 TRAINING SETUP

For frontend encoder, a tri-stage learning rate scheduler is applied with a max learning rate of $6e-5$, which is identical to the training setting used in ReVISE (Hsu et al., 2023). AdamW optimizer is used with $\beta_1=0.9$ and $\beta_2=0.98$. We optimize the frontend encoder for at most 45k updates per GPU and freeze AV-HuBERT for first 5k updates of training to warm up the conformer module. We apply the batch size of 10 on each GPU.

For vocoder training, we apply the setup of van Niekerk et al. (2021) and train vocoders with AdamW optimizer with weight decay of $1e-5$, $\beta_1=0.8$ and $\beta_2=0.99$. Exponential learning rate scheduler is applied with a decay rate of 0.999 for both the generator and the discriminators. Learning rate is set to be $1e-4$. We apply the batch size of 8 on each GPU.

For vocoder training used for zero-shot scenario and frontend encoder training both take 8 RTX4090 GPUs to run for about 24 hours. Finetuning the vocoder takes only 1 GPU with identical settings to aforementioned setup.

B EFFECT OF CONFORMER MODULE

In addition to using the AV-HuBERT frontend encoder backbone from ReVISE (Hsu et al., 2023), we also incorporate a conformer module (similar to the approach in Mira et al. (2022)) following AV-HuBERT. This module helps to smooth the transition between the visual representations and the final prediction of acoustic units in the frontend encoder. To validate its effectiveness, we conducted a comparison (Table 7), which demonstrates performance improvements with the conformer. Based on these results, we include the conformer in our experimental setup.

756
757
758
759
760
761
762
763
764
765
766
767
768
769
770
771
772
773
774
775
776
777
778
779
780
781
782
783
784
785
786
787
788
789
790
791
792
793
794
795
796
797
798
799
800
801
802
803
804
805
806
807
808
809

Models	Sync		Match	Low-Level		Qual.	Cont.
	LSE-C ↑	LSE-D ↓	SECS ↑	ESTOI ↑	MCD ↓	NISQA-MOS ↑	WER ↓
ReVISE w/o Conformer	7.11	7.20	53.84	0.290	10.71	4.09	36.27
ReVISE w/ Conformer	7.14	7.19	53.93	0.300	10.68	4.10	35.67
Proposed w/o Conformer	7.42	6.91	61.31	0.298	8.40	2.74	37.51
Proposed w/ Conformer	7.45	6.89	61.23	0.331	8.38	2.76	36.81

Table 7: Effect of Conformer module for ReVISE and proposed method on LRS3-TED dataset.